Numerical computation of dichotomy rates and projectors in discrete time

Thorsten Hüls[*]

Fakultät für Mathematik, Universität Bielefeld
Postfach 100131, 33501 Bielefeld, Germany
`huels@math.uni-bielefeld.de`

December 10, 2008

Abstract

We introduce a characterization of exponential dichotomies for linear difference equations that can be tested numerically and enables the approximation of dichotomy rates and projectors with high accuracy. The test is based on computing the bounded solutions of a specific inhomogeneous difference equation. For this task a boundary value and a least squares approach is applied. The results are illustrated using Hénon's map. We compute approximations of dichotomy rates and projectors of the variational equation, along a homoclinic orbit and an orbit on the attractor as well as for an almost periodic example. For the boundary value and the least squares approach, we analyze in detail errors that occur, when restricting the infinite dimensional problem to a finite interval.

Keywords: Exponential dichotomy, Dichotomy projectors, Boundary value problem, Least squares solution.

AMS subject classification: 34D09, 37C75, 34B05.

1 Introduction

Hyperbolicity of the linear difference equation

$$u_{n+1} = A_n u_n, \quad n \in \mathbb{Z}, \quad A_n \in \mathbb{R}^{k,k}, \quad A_n \text{ invertible,} \tag{1}$$

can be expressed in terms of an exponential dichotomy, see [8, 12, 16]. At each time n, an exponential dichotomy defines a splitting into two subspaces, in which the solution decays exponentially fast in forward- and backward-time, respectively.

Denote by Φ the solution operator of (1), defined as

$$\Phi(n, m) := \begin{cases} A_{n-1} \ldots A_m, & \text{for } n > m, \\ I, & \text{for } n = m, \\ A_n^{-1} \ldots A_{m-1}^{-1}, & \text{for } n < m. \end{cases}$$

Definition 1 *The linear difference equation (1) possesses an **exponential dichotomy** with data $(K, \alpha_s, \alpha_u, P_n^s, P_n^u)$ on $J \subset \mathbb{Z}$, if there exist two families of projectors P_n^s and $P_n^u = I - P_n^s$ and constants K, α_s, $\alpha_u > 0$, such that the following statements hold:*

$$P_n^s \Phi(n, m) = \Phi(n, m) P_m^s \quad \forall n, m \in J, \tag{2}$$

$$\begin{aligned} \|\Phi(n, m) P_m^s\| &\leq K e^{-\alpha_s(n-m)} \\ \|\Phi(m, n) P_n^u\| &\leq K e^{-\alpha_u(n-m)} \end{aligned} \quad \forall n \geq m, \ n, m \in J.$$

A typical example, where exponential dichotomies have a geometric interpretation, is a diffeomorphism $f : \mathbb{R}^k \to \mathbb{R}^k$ having a fixed point ξ and a homoclinic orbit $\bar{x}_\mathbb{Z} = (\bar{x}_n)_{n \in \mathbb{Z}}$ with respect to this fixed point, i.e. $\lim_{n \to \pm\infty} \bar{x}_n = \xi$. This orbit is called transversal, if stable and unstable manifolds of ξ intersect transversally. Equivalence of this transversality assumption to an exponential dichotomy on $\mathbb{Z}$ of the variational equation

$$u_{n+1} = Df(\bar{x}_n)u_n, \quad n \in \mathbb{Z} \tag{3}$$

is well known, see [16]. In a non-autonomous setup, in which f_n depends on n, the same connection between transversality of fiber bundles and an exponential dichotomy of the variational equation holds true, when considering homoclinic trajectories, cf. [18, 13].

Therefore, the approximation of dichotomy rates and dichotomy projectors is an important task, which we face in this paper from a numerical point of view. First we note, that it is not our attention to find a computer assisted proof of an exponential dichotomy, like, for example, the rigorous computational shadowing results, introduced in [7]. For an arbitrary sequence of matrices $A_\mathbb{Z} = (A_n)_{n \in \mathbb{Z}}$, a computer assisted proof of an exponential dichotomy on $\mathbb{Z}$ is impossible without having further structural information. Numerically, one can only compute on finite intervals $J = [n_-, n_+] \cap \mathbb{Z}$. But if (1) possesses an exponential dichotomy on J, it does not necessarily has one on $\mathbb{Z}$. A counterexample is $A_n = I$ for $n \notin J$. On the other hand, an exponential dichotomy on $\mathbb{Z}$ follows for almost periodic systems from an exponential dichotomy on a sufficiently large interval, see for example [1, 17]. Further note that for linear upper triangular ODEs, techniques for computing Sacker-Sell

spectral intervals are introduced in [9], that are based on the relationships between different spectra.

In Section 2, we first prove that the dichotomy rates are related to the exponential rates of decay of the solution of the inhomogeneous equation

$$u_{n+1} = A_n u_n + \delta_{n,N} r, \quad r \in \mathbb{R}^k, \quad n \in \mathbb{Z}, \tag{4}$$

where $\delta_{n,m}$ is the Kronecker symbol. This result is applied in Section 3, to develop an algorithm for approximating dichotomy rates and the corresponding dichotomy projectors. Here it is crucial to solve system (4) on finite intervals with high accuracy. For this task, two different approaches are introduced. The first one is based on solving linear boundary value problems while the second one computes least squares solutions, see also [5] where similar techniques apply for a global error analysis of initial value ODEs.

As a toy model, Hénon's map is used. We approximate dichotomy rates of the variational equation (3), where $\bar{x}_{\mathbb{Z}}$ is a transversal or tangential homoclinic orbit, a sequence on the Hénon attractor or an almost periodic bounded trajectory.

Approximation errors of the solution of (4) on finite intervals are discussed in Section 4. For the boundary value approach, we analyze the influence of the chosen boundary operator. Furthermore, we show that effects, caused by matrices outside the finite interval J, decay exponentially fast. For the least squares approach, we prove an exponential estimate for the approximation error.

2   Computing dichotomy rates

In [12, Theorem 7.6.5], Henry proved that (1) possesses an exponential dichotomy on $\mathbb{Z}$, if and only if the inhomogeneous equation

$$u_{n+1} = A_n u_n + r_n, \quad n \in \mathbb{Z}$$

has for each bounded sequence $r_{\mathbb{Z}} := (r_n)_{n \in \mathbb{Z}}$ a unique bounded solution, see also [6].

In this section, we give a modified result that allows the numerical computation of the corresponding dichotomy rates.

Theorem 2 *Assume that A_n is invertible for all $n \in \mathbb{Z}$. Then the following assertions are equivalent.*

(i) The inhomogeneous equation

$$u_{n+1} = A_n u_n + \delta_{n,N} r, \quad n \in \mathbb{Z} \tag{5}$$

possesses for all $N \in \mathbb{Z}$ and $r \in \mathbb{R}^k$ a unique bounded solution, fulfilling

$$\|u_n\| \leq \begin{cases} K \mathrm{e}^{-\alpha_s(n-N-1)} \|r\|, & \text{for } n \geq N+1, \\ K \mathrm{e}^{-\alpha_u(N+1-n)} \|r\|, & \text{for } n \leq N. \end{cases} \tag{6}$$

(ii) The difference equation (1) possesses an exponential dichotomy on $\mathbb{Z}$ with dichotomy constants K, α_s, α_u.

Proof: Assume (i) and denote by Φ the solution operator of (1). Since (5) has for each $r \in \mathbb{R}^k$ and $N \in \mathbb{Z}$ a unique bounded solution, the homogeneous equation has no non-trivial bounded solution. We define the subspaces

$$
\begin{aligned}
S^+ &= \left\{ x : \sup_{n \geq 0} \|\Phi(n,0)x\| < \infty \right\}, \\
S^- &= \left\{ x : \sup_{n \leq 0} \|\Phi(n,0)x\| < \infty \right\}
\end{aligned}
$$

and it follows that $S^+ \cap S^- = \{0\}$ and $S^+ \oplus S^- = \mathbb{R}^k$. Let P_0^s be the projector with $\mathcal{R}(P_0^s) = S^+$ and $\mathcal{N}(P_0^s) = S^-$. The complementary projector is given as $P_0^u := I - P_0^s$ and

$$
P_n^{s,u} := \Phi(n,0) P_0^{s,u} \Phi(0,n), \quad n \in \mathbb{Z}.
$$

A solution of (5) can be constructed, using Green's function, see [16]

$$
u_n = G(n, N+1)r, \quad n \in \mathbb{Z}, \tag{7}
$$

where G is defined as

$$
G(n,m) = \begin{cases} \Phi(n,m)P_m^s, & n \geq m, \\ -\Phi(n,m)P_m^u, & n < m. \end{cases} \tag{8}
$$

By construction

$$
u_n \in \begin{cases} \mathcal{R}(P_n^s), & \text{for } n \geq N+1, \\ \mathcal{R}(P_n^u), & \text{for } n < N+1 \end{cases}
$$

and as a consequence, $u_{\mathbb{Z}}$ is the unique bounded solution that converges by assumption (6) exponentially fast to 0.

It holds for $n \geq N+1$

$$
\|u_n\| = \|\Phi(n, N+1)P_{N+1}^s r\| \leq K\mathrm{e}^{-\alpha_s(n-N-1)}\|r\|, \quad r \in \mathbb{R}^k,
$$

and therefore

$$
\|\Phi(n, N+1)P_{N+1}^s\| \leq K\mathrm{e}^{-\alpha_s(n-N-1)}. \tag{9}
$$

This proves the first dichotomy estimate, since (9) holds for all $N \in \mathbb{Z}$.

The second dichotomy estimate follows from

$$
\|u_n\| = \|\Phi(n, N+1)P_{N+1}^u r\| \leq K\mathrm{e}^{-\alpha_u(N+1-n)}\|r\| \quad \text{for } n < N+1 \text{ and all } N \in \mathbb{Z}.
$$

Thus, (1) possesses an exponential dichotomy on $\mathbb{Z}$ with data $(K, \alpha_s, \alpha_u, P_n^s, P_n^u)$.

Using the explicit solution (7), it immediately follows, that the converse also holds true.

$\blacksquare$

Note that due to linearity, it suffices to consider statement (i) for vectors r from a basis of $\mathbb{R}^k$. However, for the numerical tests in Section 3 we only take one generic vector r, which we choose at random.

Approximations of dichotomy projectors can be computed, by solving inhomogeneous linear systems.

Corollary 3 *Let condition (i) from Theorem 2 be fulfilled. Fix $N \in \mathbb{Z}$ and let $u_{\mathbb{Z}}^i$ be the solution of (5) for $r = e_i$, $i = 1, \ldots, k$, where e_i is the i-th unit vector.*

Then (1) possesses an exponential dichotomy on $\mathbb{Z}$ with stable projector

$$P_{N+1}^s = \begin{pmatrix} u_{N+1}^1 & u_{N+1}^2 & \cdots & u_{N+1}^k \end{pmatrix}.$$

Proof: For each $i = 1, \ldots, k$, the solution $u_{\mathbb{Z}}^i$ of

$$u_{n+1} = A_n u_n + \delta_{n,N} e_i, \quad n \in \mathbb{Z}$$

has the explicit form, see (7)

$$u_n^i = G(n, N+1) e_i, \quad n \in \mathbb{Z},$$

and using (8), we get

$$u_{N+1}^i = P_{N+1}^s e_i.$$

■

Finally, we analyze, whether two half-sided dichotomies on $\mathbb{Z}^+$ and $\mathbb{Z}^-$ with projectors of equal rank, lead to an exponential dichotomy on $\mathbb{Z}$. Note that the variational equation (3) along a tangential homoclinic orbit possesses half sided dichotomies on $\mathbb{Z}^+$ and $\mathbb{Z}^-$, but no exponential dichotomy on $\mathbb{Z}$.

Proposition 4 *Assume that the homogeneous difference equation (1) possesses an exponential dichotomy on $\mathbb{Z}^+$ and $\mathbb{Z}^-$ with projectors of equal rank. Then (1) has an exponential dichotomy on $\mathbb{Z}$ if and only if the inhomogeneous equation (5) has a bounded solution for $N = 0$ and all $r \in \mathbb{R}^k$.*

Proof: Let $u_{\mathbb{Z}}$ be a bounded solution of (5) on $\mathbb{Z}$. To obtain a contradiction, suppose that the homogeneous equation (1) has non-trivial bounded solutions on $\mathbb{Z}$ which is equivalent to, see [16, Proposition 2.3]

$$\dim \left(\mathcal{R}(P_0^{+s}) \cap \mathcal{R}(P_0^{-u}) \right) \geq 1,$$

where $P_n^{+s,u}$ and $P_n^{-s,u}$ denote the stable and unstable dichotomy projectors of (1) on $\mathbb{Z}^+$ and $\mathbb{Z}^-$, respectively.

Due to boundedness and the cocycle property (2) of dichotomy projectors we get

$$A_0 u_0 + r = u_1 = P_1^{+s} u_1 = P_1^{+s}(A_0 u_0 + r) \quad \text{and} \quad P_0^{-u} u_0 = u_0,$$

and therefore

$$
\begin{aligned}
& P_1^{+s}(A_0 u_0 + r) = A_0 P_0^{-u} u_0 + r \\
\Leftrightarrow\ & P_0^{+s} u_0 + P_0^{+s} A_0^{-1} r = P_0^{-u} u_0 + A_0^{-1} r \\
\Leftrightarrow\ & (P_0^{+s} - P_0^{-u}) u_0 = -P_0^{+s}\tilde{r} + \tilde{r} \in \mathcal{N}(P_0^{+s}), \quad \text{where } \tilde{r} = A_0^{-1} r. \qquad (10)
\end{aligned}
$$

Since

$$
\mathcal{R}(P_0^{+s}) + \mathcal{R}(P_0^{-u}) \not\subset \mathcal{N}(P_0^{+s})
$$

it follows that in general, an u_0, fulfilling (10), does not exist, and as a consequence, the inhomogeneous equation has not for all $r \in \mathbb{R}^k$ a bounded solution.

Thus, $\mathcal{R}(P_0^{+s}) \cap \mathcal{R}(P_0^{-u}) = \{0\}$ and we obtain an exponential dichotomy on $\mathbb{Z}$. The converse is a direct consequence of Theorem 2.

∎

The dichotomy test in Section 3 is based on Theorem 2. In order to prove an exponential dichotomy, we first have to check, if condition (6) holds true. This is realized in Section 3, by solving (5) on a finite interval. The logarithmic slope of the solution then gives approximations of the dichotomy constants α_u and α_s. For an approximation of dichotomy projectors with high accuracy, we use the idea, introduced in Corollary 3.

3 Numerical computations

Given a sequence of matrices $A_J = (A_n)_{n \in J}$, $A_n \in \mathbb{R}^{k,k}$, we compute approximations of dichotomy constants and projectors of (1) as follows:

(i) Solve (5) on a sufficiently large interval J.

(ii) Determine the exponential slope of the solution.

For the main task (i), we introduce two different approaches. We compute finite approximations applying a boundary value and a least squares ansatz, respectively.

3.1 A boundary value approach

The boundary value approach requires to solve the following linear equations on the finite interval $J = [n_-, n_+]$:

$$
\begin{aligned}
u_{n+1} &= A_n u_n + c \cdot \delta_{n,N} r, \quad n = n_-, \ldots, n_+ - 1, & (11) \\
b(u_{n_-}, u_{n_+}) &= 0, & (12) \\
\sum_{i=n_-}^{n_+} u_i^T \mathbb{1} &= 1. & (13)
\end{aligned}
$$

In (11), an extra variable c is introduced, to determine whether the homogeneous equation possesses a non-trivial bounded solution, see Proposition 4. The normalizing condition (13) is needed to get a square system. Finally, $b : \mathbb{R}^{2k} \to \mathbb{R}^k$ is an appropriately chosen boundary operator. The concrete choice of boundary conditions and corresponding approximation results are discussed in Section 4. If the boundary operator is linear, system (11)-(13) may equivalently be written as

$$
\begin{pmatrix}
-A_{n_-} & I & & & & & 0 \\
& \ddots & \ddots & & & & \vdots \\
& & \ddots & \ddots & & & -r \\
& & & \ddots & \ddots & & \vdots \\
& & & & -A_{n_+-1} & I & 0 \\
D_1 b & & & & & D_2 b & 0 \\
1 & 1 & \dots & \dots & \dots & 1 & 0
\end{pmatrix}
\begin{pmatrix}
u_{n_-} \\ \vdots \\ \vdots \\ \vdots \\ \vdots \\ u_{n_+} \\ c
\end{pmatrix}
=
\begin{pmatrix}
0 \\ \vdots \\ \vdots \\ \vdots \\ \vdots \\ 0 \\ 1
\end{pmatrix}.
\tag{14}
$$

For the infinite dimensional problem (5), the dichotomy rates can be computed, by Theorem 2, from the logarithmic slope of the solution of (14). We use this idea also for our finite dimensional approximations and present its formal justification in Section 4.

3.2   A least squares approach

Assume that the homogeneous equation possesses an exponential dichotomy on $\mathbb{Z}$. As an alternative to the boundary value approach, we compute the least squares solution of

$$
u_{n+1} = A_n u_n + \delta_{n,N} r, \quad n \in J = [n_-, n_+], \quad N \in J,
\tag{15}
$$

and approximate dichotomy rates in a second step. System (5) can equivalently be written as $Bu = R$, where

$$
B = \begin{pmatrix}
-A_{n_-} & I & & \\
& \ddots & \ddots & \\
& & -A_{n_+-1} & I
\end{pmatrix}, \quad
u_J = \begin{pmatrix} u_{n_-} \\ \vdots \\ u_{n_+} \end{pmatrix}, \quad
R_i = \begin{cases} 0, & i \in J, \; i \neq N, \\ r, & i = N, \end{cases}
$$

and we seek for the solution, that is minimal w.r.t. $\| \cdot \|_2$. The least squares solution $\bar{u}_J$ of (15) is $\bar{u}_J = B^+ R$, and since B has full rank, the Moore-Penrose inverse B^+ can be computed as

$$
B^+ = B^T (BB^T)^{-1},
$$

see [19]. Note that BB^T is a sparse matrix with a block-tridiagonal structure, which one can invert efficiently.

Errors between the unique bounded solution on $\mathbb{Z}$ and the finite least squares approximation, are discussed in Section 4.2.

3.3 Dichotomy rates along a homoclinic orbit

For numerical computations, we consider the well known Hénon map [11]

$$f(x) = \begin{pmatrix} 1 + x_2 - ax_1^2 \\ bx_1 \end{pmatrix} \qquad \text{with parameters} \qquad a = 1.4, \ b = 0.3, \qquad (16)$$

and compute a homoclinic orbit $\bar{x}_{n+1} = f(\bar{x}_n)$, $n \in \mathbb{Z}$ with respect to the fixed point

$$\xi = \begin{pmatrix} z \\ bz \end{pmatrix} \quad \text{where} \quad z = \frac{b - 1 + \sqrt{(b-1)^2 + 4a}}{2a},$$

i.e. $\lim_{n \to \pm\infty} \bar{x}_n = \xi$, cf. [3]. Then our method applies to the variational equation

$$u_{n+1} = Df(\bar{x}_n)u_n, \quad n \in \mathbb{Z}. \qquad (17)$$

Note that the matrix $Df(\xi)$ has one stable and one unstable eigenvalue λ_s and λ_u, respectively. Therefore, the difference equation

$$u_{n+1} = Df(\xi)u_n, \quad n \in \mathbb{Z}$$

possesses an exponential dichotomy on $\mathbb{Z}$ with dichotomy rates

$$\bar{\alpha}_s = -\log|\lambda_s|, \quad \bar{\alpha}_u = \log|\lambda_u|. \qquad (18)$$

Furthermore, $Df(\bar{x}_n)$ converges exponentially fast towards $Df(\xi)$ as $n \to \pm\infty$, see Figure 2. An $\mathcal{L}_1$ roughness-theorem applies, see [8, 2] and we obtain exponential dichotomies on $\mathbb{Z}^-$ and $\mathbb{Z}^+$ of (17) with the same exponential rates $\bar{\alpha}_s$, $\bar{\alpha}_u$. Since stable and unstable manifolds of ξ intersect transversally, [16, Proposition 2.6] proves an exponential dichotomy of (17) on $\mathbb{Z}$ with rates $\bar{\alpha}_s$, $\bar{\alpha}_u$.

We compare these exact values with numerical approximations. On the interval $J = [-100, 100]$ a homoclinic orbit is computed, using the techniques introduced in [4], see Figure 1 (left). In a second step, we solve (14) for $N = 0$ and plot its solution u_J in Figure 1 (right) in a logarithmic scale.

Due to Theorem 2, the dichotomy rates α_s and α_u are the slopes the solution u_J. To obtain an approximation of α_s, we take points $(n, \log(\|u_n\|))$ such that $n \geq 3$ and $\|u_n\| > 10^{-14}$. By a least squares approach, we fit these points and get α_s as the slope of the resulting line. For α_u, the same approach is applied for $n < 2$. The resulting rates are $\alpha_s = 1.85803258$ and $\alpha_u = 0.65401$ when computing u_J via the boundary value approach, while $\alpha_s = 1.85803259$ and $\alpha_u = 0.65402$ in case of minimizing. On the other hand, the exact dichotomy rates from (18) are $\bar{\alpha}_s = 1.858243418746994$ and $\bar{\alpha}_u = 0.6542706144210578$, thus the difference between theoretical and numerical results is of order 10^{-4}.

The constant c from (11) indicates transversality, and its value is $c = -0.971$.

Now we vary N and discuss the dependence of errors for α_u, α_s. For $N = -20$ the solution of (14) looks similar to Figure 1 (right), where the peak is shifted to $n = -20$.
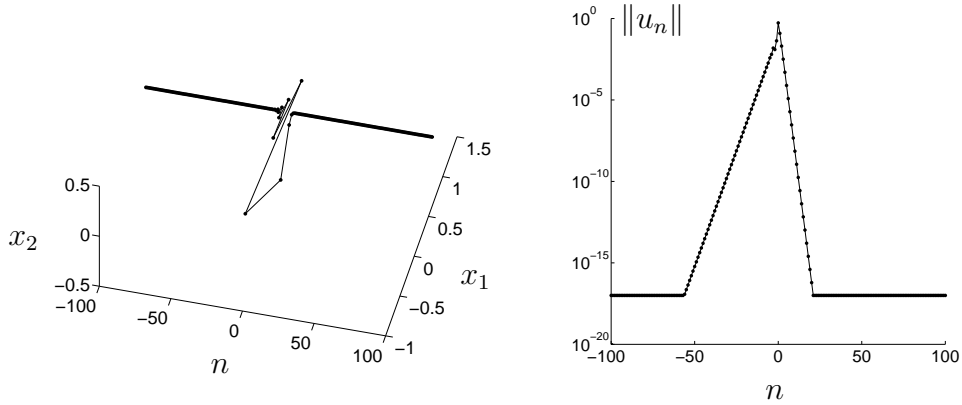
Figure 1: *A homoclinic orbit x_J of (16) (left) and the solution u_J of (14), plotted over n in a logarithmic scale, where $N = 0$, $A_n = Df(x_n)$, $n \in J$ (right).*
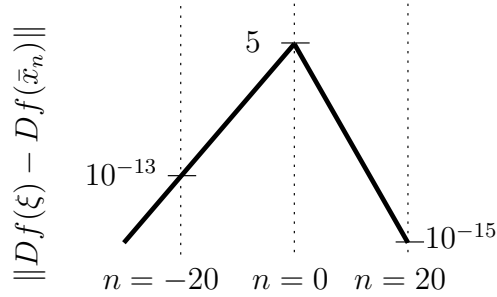

Figure 2: *Exponentially fast convergence of $Df(\bar{x}_n)$ to $Df(\xi)$.*

Since $\|Df(\xi) - Df(\bar{x}_n)\|$ converges exponentially fast to 0, see Figure 2, the equation

$$u_{n+1} = Df(\bar{x}_n)u_n + \delta_{n,-20}r$$

is for $n \leq -20$ nearly a constant coefficient problem. Thus the computation of α_u yields better results for $N = -20$ than for $N = 0$. On the other hand, the influence of the non-constant matrices $Df(\bar{x}_n)$, $|n|$ small, results in a worse approximation of α_s. Numerically, we obtain

$$|\alpha_u - \bar{\alpha}_u| \approx 10^{-9}, \quad |\alpha_s - \bar{\alpha}_s| \approx 10^{-2}.$$

A computation for $N = 20$ gives an opposite result.

Note that one should not solve (14) for N close to $n_\pm$, since extra points on both sides of N are needed for an approximation of the dichotomy rates.

9

3.4 Approximation of dichotomy projectors

For the example from Section 3.3, the corresponding dichotomy projectors P_0^s are approximated numerically. Following the approach, introduced in Corollary 3, we fix $N = -1$ and solve (11)-(13) for $r = e_1$ and $r = e_2$ on the interval $J = [-100, 100]$. Denote by (u_J^1, c^1) and (u_J^2, c^2) the corresponding solutions. We compensate the scaling factors c^1, c^2 and define

$$P_0^s := \left(\frac{1}{c^1} \cdot u_0^1 \qquad \frac{1}{c^2} \cdot u_0^2 \right).$$

Note that if one neglects the test for transversality, one can directly solve the inhomogeneous system (11), (12) with fixed $c = 1$, and right hand sides $r = e_1$ and $r = e_2$, respectively.

Alternatively, the least squares solution of (15) can be computed for $r = e_1$ and $r = e_2$.

Numerically, we get in all cases

$$P_0^s = \begin{pmatrix} -0.132377157578668 & 1.014597654357702 \\ -0.147744151372172 & 1.132377157578668 \end{pmatrix}. \tag{19}$$

For testing whether P_0^s is a precise approximation of the stable dichotomy projector, we first note that $\|P_0^s \cdot P_0^s - P_0^s\|_2 = 2.8 \cdot 10^{-17}$. Secondly, take a random vector v, define $u_0 = P_0^s v$, and compute the iterates $u_{n+1} = Df(\bar{x}_n)u_n$ for $n = 0, \dots, 19$, see Table 1.

n	$\|u_n\|_2$	$\log(\|u_n\|/\|u_{n-1}\|)$	n	$\|u_n\|_2$	$\log(\|u_n\|/\|u_{n-1}\|)$
0	6.59e-01		10	7.43e-09	-1.85824334
1	1.27e-01	-1.47308036	11	1.16e-09	-1.85824420
2	2.10e-02	-1.80148137	12	1.81e-10	-1.85823370
3	3.31e-03	-1.84948746	13	2.82e-11	-1.85836329
4	5.16e-04	-1.85688031	14	4.40e-12	-1.85675690
5	8.05e-05	-1.85803090	15	6.75e-13	-1.87534346
6	1.26e-05	-1.85821028	16	1.45e-13	-1.53695258
7	1.96e-06	-1.85823825	17	1.30e-13	-0.110845343
8	3.05e-07	-1.85824261	18	2.59e-13	0.690491431
9	4.76e-08	-1.85824330	19	4.96e-13	0.650758902

Table 1: *Norm of the iterates u_n, $n = 0, \dots, 19$ and logarithmic rates of decay.*

In a hyperbolic system, the iteration of points from the stable subspace is highly sensitive to rounding errors. Thus the results in Table 1 suggest, that the approximation of the dichotomy projector is exact up to machine accuracy. This result is formalized in Section 4.1.3.

3.5 Hyperbolic almost periodic bounded sequences

Consider the non-autonomous difference equation

$$\bar{x}_{n+1} = f(\bar{x}_n, a_n), \quad f(x, a) = \begin{pmatrix} 1 + x_2 - ax_1^2 \\ bx_1 \end{pmatrix}, \quad b = 0.3, \quad n \in \mathbb{Z}, \qquad (20)$$

where $a_n = 1.4 + \frac{1}{2}\sin(\frac{1}{5}n)$ is an almost periodic sequence of parameters.

We compute on the interval $J = [-500, 500]$ a finite solution $\bar{x}_J$ of (20), see Figure 3 (left), using the algorithm that is introduced in [14]. Consequently, the variational equation along this orbit is almost periodic. The solution of the inhomogeneous problem

$$u_{n+1} = Df(\bar{x}_n, a_n)u_n + \delta_{n,N}r, \quad n \in J \qquad (21)$$

is shown for $N = 0$ in the right diagram of Figure 3, and the corresponding dichotomy rates are $\alpha_s = 2.465768$, $\alpha_u = 1.265891$. To analyze the dependence of
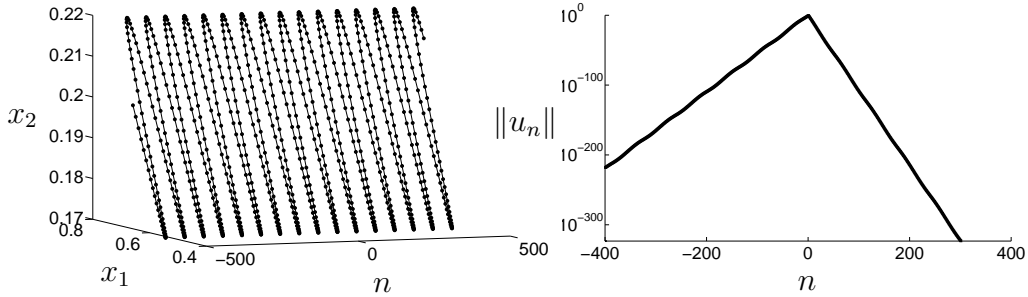

Figure 3: *Bounded solution of (20) (left) and the solution of (21) (right) plotted in a logarithmic scale.*

these rates on the chosen N, cf. Theorem 2, we compute α_s, α_u for $N \in [-400, 400]$, see Figure 4.
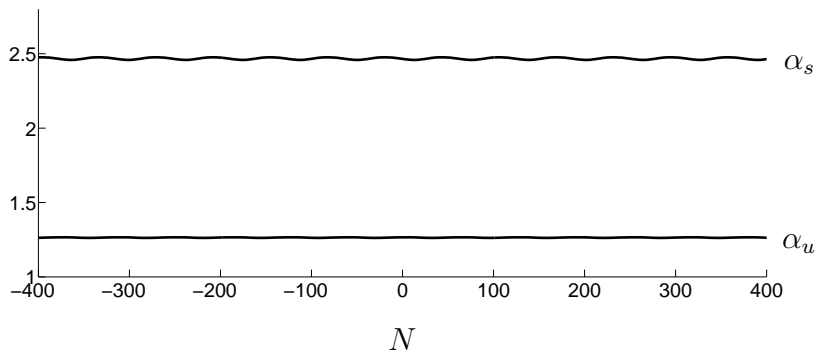

Figure 4: *Approximation of α_s and α_u for $N \in [-400, 400]$, using the boundary value approach.*

11

Note that an exponential dichotomy on a sufficiently large interval J guarantees for almost periodic systems the existence of an exponential dichotomy on $\mathbb{Z}$, see [1, 17].

3.6 Hyperbolic sequences on the Hénon attractor

We analyze, if a sequence on the Hénon attractor for the classical parameters $a = 1.4$, $b = 0.3$ is hyperbolic, i.e. the variational equation along this sequence possesses an exponential dichotomy. In the first step, a sequence on the attractor is constructed by iteration. We iterate 100 steps for an appropriate initial vector, to reach the attractor, and save the next 1001 steps in $\bar{x}_n$, $n = -500, \ldots 500$.
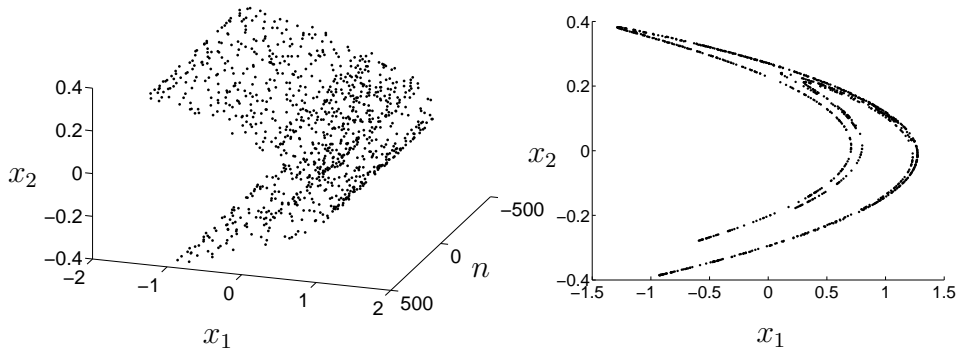

Figure 5: *An orbit of length* 1001 *on the Hénon attractor, plotted over its index n (left), and in phase space (right).*

With $A_n = Df(\bar{x}_n)$, we then solve (5) for $N = 0$, see Figure 6, and the resulting dichotomy rates are $\alpha_s = 1.66$ and $\alpha_u = 0.39$.
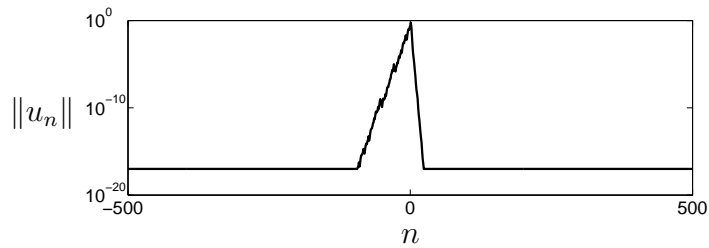

Figure 6: *Solution u_J of (14), plotted over n in a logarithmic scale.*

The dependence of α_s, α_u on the chosen N is shown in Figure 7. Here, boundary value and least squares approach lead to nearly identical results.

Since r is chosen at random, and therefore has a generic position, our computations suggest that the variational equation possesses an exponential dichotomy on the finite interval $[-400, 400]$.
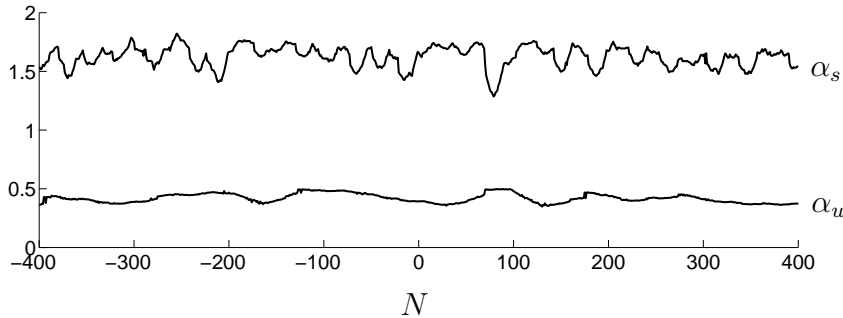
12

Figure 7: *Approximation of α_s and α_u for $N = -400, \ldots, 400$, using the boundary value approach.*

Note that we cannot conclude from this result that Hénon's attractor is hyperbolic. Although the chosen trajectory lies dense on the attractor as $J \to \mathbb{Z}$, it does not contain, all bounded trajectories, as periodic orbits, for example.

3.7 A tangential homoclinic orbit

Consider parameters for which tangential homoclinic orbits of Hénon's map exist. In this case, the variational equation (17) possesses exponential dichotomies on $\mathbb{Z}^-$ and $\mathbb{Z}^+$ but no dichotomy on $\mathbb{Z}$, since (17) has non-trivial bounded solutions, cf. [15, 3]. In this case, the value of the constant c in (11) should be 0, cf. Proposition 4.

For the parameters $a = 1.4$ and $b = 0.1014563589$ in Hénon's map, we are close to a homoclinic tangency. When solving (14) on the interval $J = [-200, 200]$ with $N = 0$, we obtain a transversality constant c of magnitude 10^{-4}, and an error in the dichotomy rates $|\alpha_{s,u} - \bar{\alpha}_{s,u}|$ of order 10^{-3}.

4 Justification of the numerical process

In Sections 3.1, 3.2 two approaches are introduced for getting finite approximations of the solution of (5). In both cases, we will present a detailed error analysis under the assumption that the homogeneous difference equation possesses an exponential dichotomy on $\mathbb{Z}$.

A1 The linear difference equation

$$u_{n+1} = A_n u_n, \quad n \in \mathbb{Z} \tag{22}$$

with uniformly bounded invertible matrices A_n, possesses an exponential dichotomy on $\mathbb{Z}$ with data $(K, \alpha_s, \alpha_u, P_n^s, P_n^u)$.

13

4.1 The boundary value approach

By assuming an exponential dichotomy on $\mathbb{Z}$, the free variable c in (11) that tests for transversality, is not needed and thus, the normalizing condition (13) also vanishes. When choosing a linear boundary operator, (14) reduces to

$$
\begin{pmatrix}
-A_{n_-} & I & & & \\
& \ddots & \ddots & & \\
& & \ddots & \ddots & \\
& & & -A_{n_+-1} & I \\
D_1 b & & & & D_2 b
\end{pmatrix}
\begin{pmatrix}
u_{n_-} \\ \vdots \\ \vdots \\ \vdots \\ \vdots \\ u_{n_+}
\end{pmatrix}
=
\begin{pmatrix}
0 \\ \vdots \\ r \\ \vdots \\ 0
\end{pmatrix}.
\tag{23}
$$

We analyze errors that occur, when solving this finite dimensional problem (23) instead of the infinite dimensional system (22).

4.1.1 Effects of matrices with large $|n|$

Let J be a finite interval. Note that the system (23) does not depend on the matrices A_n, for which n lies outside the interval J. Thus no matter how A_n is defined for $n \notin J$, we always obtain the same finite approximation. Fortunately, the influence from the outer matrices decays exponentially fast towards the middle of the interval J. This is proven for non-autonomous systems, generated by a parameter dependent non-linear map, in [14, Theorem 4]. Here, we state the corresponding linear result.

Proposition 5 *Assume **A1**. Let J be a finite interval and let $B_{\mathbb{Z}}^J$ be a family of matrix sequences, fulfilling $B_n^J = A_n$, for $n \in J$. Assume that the difference equation*

$$
v_{n+1} = B_n^J v_n, \quad n \in \mathbb{Z}
$$

possesses for each J an exponential dichotomy on $\mathbb{Z}$ with J-independent constants L, β_s, β_u.

For $N \in J$ and $r \in \mathbb{R}^k$ denote by $\bar{u}_{\mathbb{Z}}$ and $\bar{v}_{\mathbb{Z}}$ the unique bounded solutions of

$$
\begin{aligned}
\bar{u}_{n+1} &= A_n \bar{u}_n + \delta_{n,N} r, \quad n \in \mathbb{Z}, \\
\bar{v}_{n+1} &= B_n^J \bar{v}_n + \delta_{n,N} r, \quad n \in \mathbb{Z}.
\end{aligned}
$$

Then there exists a J-independent positive constant C, such that the following estimate holds for $n \in J = [n_-, n_+]$

$$
\|\bar{u}_n - \bar{v}_n\| \leq C \left(e^{-\alpha_s(n-n_-)} e^{-\beta_u(N-n_-)} + e^{-\alpha_u(n_+-n)} e^{-\beta_s(n_+-N)} \right).
$$

Proof: For $n \in \mathbb{Z}$ define $d_n := \bar{u}_n - \bar{v}_n$. Then

$$
\begin{aligned}
d_{n+1} &= \bar{u}_{n+1} - \bar{v}_{n+1} = A_n \bar{u}_n - B_n^J \bar{v}_n = A_n(\bar{u}_n - \bar{v}_n) + (A_n - B_n^J)\bar{v}_n \\
&= A_n d_n + q_n,
\end{aligned}
$$

14

where $q_n = \begin{cases} 0, & n \in J, \\ A_n \bar{v}_n - \bar{v}_{n+1}, & n \notin J. \end{cases}$

Since (22) possesses an exponential dichotomy on $\mathbb{Z}$, the unique bounded solution of

$$x_{n+1} = A_n x_n + q_n \tag{24}$$

is

$$x_n = \sum_{m \in \mathbb{Z}} G(n, m+1) q_m,$$

where Green's function G is defined in (8).

By Theorem 2 and since A_n is uniformly bounded, there exists a constant $\tilde{C} > 0$, such that

$$\|q_n\| \leq \begin{cases} \tilde{C} \mathrm{e}^{-\beta_s(n-N-1)}, & n > n_+, \\ \tilde{C} \mathrm{e}^{-\beta_u(N+1-n)}, & n < n_-, \\ 0 & n_- \leq n \leq n_+. \end{cases}$$

Using the dichotomy estimates, we get for $n \in J$

$$\begin{aligned}
\|x_n\| &\leq \sum_{m \in \mathbb{Z}} \|G(n, m+1) q_m\| \\
&= \sum_{m=-\infty}^{n_- - 1} \|G(n, m+1) q_m\| + \sum_{m=n_+ + 1}^{\infty} \|G(n, m+1) q_m\| \\
&\leq \sum_{m=-\infty}^{n_- - 1} \|\Phi(n, m+1) P_{m+1}^s q_m\| + \sum_{m=n_+ + 1}^{\infty} \|\Phi(n, m+1) P_{m+1}^u q_m\| \\
&\leq \sum_{m=-\infty}^{n_- - 1} \tilde{C} K \mathrm{e}^{-\alpha_s(n-m-1)} \mathrm{e}^{-\beta_u(N+1-m)} + \sum_{m=n_+ + 1}^{\infty} \tilde{C} K \mathrm{e}^{-\alpha_u(m+1-n)} \mathrm{e}^{-\beta_s(m-N-1)} \\
&= \tilde{C} K \Big(\sum_{m=-\infty}^{0} \mathrm{e}^{-\alpha_s(n-m-n_-)} \mathrm{e}^{-\beta_u(N+2-n_- - m)} \\
&\quad + \sum_{m=0}^{\infty} \mathrm{e}^{-\alpha_u(m+n_+ + 2 - n)} \mathrm{e}^{-\beta_s(m+n_+ - N)} \Big) \\
&= \tilde{C} K \Big(\frac{1}{1 - \mathrm{e}^{-\alpha_s - \beta_u}} \mathrm{e}^{-\alpha_s(n-n_-)} \mathrm{e}^{-\beta_u(N-n_- + 2)} \\
&\quad + \frac{1}{1 - \mathrm{e}^{-\alpha_u - \beta_s}} \mathrm{e}^{-\alpha_u(n_+ - n + 2)} \mathrm{e}^{-\beta_s(n_+ - N)} \Big).
\end{aligned}$$

By construction, $d_{\mathbb{Z}}$ is the unique bounded solution of (24) and therefore

$$\|d_n\| \leq C \left(\mathrm{e}^{-\alpha_s(n-n_-)} \mathrm{e}^{-\beta_u(N-n_-)} + \mathrm{e}^{-\alpha_u(n_+ - n)} \mathrm{e}^{-\beta_s(n_+ - N)} \right), \quad n \in J,$$

with constant $C = \tilde{C} K \max \left\{ \frac{\mathrm{e}^{-2\beta_u}}{1 - \mathrm{e}^{-\alpha_s - \beta_u}}, \frac{\mathrm{e}^{-2\alpha_u}}{1 - \mathrm{e}^{-\alpha_u - \beta_s}} \right\}.$

∎

4.1.2 Approximation results

We show that errors of the boundary value approach essentially depend on the chosen boundary operator. Assume **A1**, and define the operator Γ on a finite interval $J = [n_-, n_+]$:

$$\Gamma_J := \begin{pmatrix} -A_{n_-} & I & & & \\ & \ddots & & \ddots & \\ & & & -A_{n_+-1} & I \\ D_1 b & & & & D_2 b \end{pmatrix}.$$

Projection boundary conditions require the following assumptions:

A2 There exist two complementary projectors Q^s and Q^u having the same rank as the stable and unstable dichotomy projectors P_n^s and P_n^u, and an angle $0 < \sigma \le \frac{\pi}{2}$ such that

$$\measuredangle(\mathcal{R}(P_{n_-}^s), \mathcal{R}(Q^u)) > \sigma, \quad \measuredangle(\mathcal{R}(P_{n_+}^u), \mathcal{R}(Q^s)) > \sigma,$$

for sufficiently large $-n_-$, n_+.

The angle between two subspaces A and B is defined as (see [10])

$$\measuredangle(A, B) = \theta \in \left[0, \frac{\pi}{2}\right], \quad \text{where} \quad \cos\theta = \max_{u \in A, \|u\|=1} \max_{v \in B, \|v\|=1} u^T v.$$

As boundary operator, we either take periodic or projection boundary conditions, defined as

$$b_{\text{per}}(x, y) \quad := \quad x - y, \tag{25}$$

$$b_{\text{proj}}(x, y) \quad := \quad \begin{pmatrix} Y_s^T x \\ Y_u^T y \end{pmatrix}, \tag{26}$$

where the columns of Y_s and Y_u form a basis of $\mathcal{R}(Q^u)^\perp$ and $\mathcal{R}(Q^s)^\perp$.

We impose the following regularity assumption, cf. [13, Lemma 4.3]:

A3 Let $b \in \mathcal{C}^1(\mathbb{R}^{2k}, \mathbb{R}^k)$, $b(0, 0) = 0$ and the operator

$$R_{n_\pm} := \left(D_1 b(0, 0)_{|\mathcal{R}(P_{n_-}^s)} \quad D_2 b(0, 0)_{|\mathcal{R}(P_{n_+}^u)} \right)$$

is invertible for sufficiently large $-n_-$, n_+, and has a uniformly bounded inverse, i.e. there exist a $C > 0$ and an $L \in \mathbb{N}$ such that

$$\|R_{n_\pm}^{-1}\| \le C \quad \text{for all} \ -n_-, \ n_+ \ge L.$$

Note that for projection boundary conditions (26), assumption **A3** directly follows from **A2**, see Appendix A, Lemma 11.

In case of periodic boundary conditions (25), **A3** is satisfied, if $\measuredangle(\mathcal{R}(P_{n_-}^s), \mathcal{R}(P_{n_+}^u)) > \tilde{\sigma}$ for some $0 < \tilde{\sigma} \le \frac{\pi}{2}$ and all sufficiently large $-n_-$, n_+.

Proposition 6 *Assume **A1**–**A3**, take a finite interval J and fix $N \in J$. Choose an $r \in \mathbb{R}^k$ and define $r_J := (0, \ldots, 0, r, 0, \ldots, 0)^T$, where r is placed at N-th position. Denote by $\bar{u}_{\mathbb{Z}}$ the unique bounded solution of the infinite dimensional problem (5) and let $\bar{u}_{|J}$ be its restriction to the finite interval J.*

Then

$$\Gamma_J u_J = r_J$$

possesses for sufficiently large intervals J a unique solution u_J and the error can be estimated as

$$\|\bar{u}_{|J} - u_J\| \leq C\|b(\bar{u}_{n_-}, \bar{u}_{n_+})\|. \tag{27}$$

Proof: By [13, Lemma 4.3] it follows that the operator Γ_J has for sufficiently large $-n_-, n_+$ a uniformly bounded inverse and consequently

$$
\begin{aligned}
\|\bar{u}_{|J} - u_J\| &\leq \|\Gamma_J^{-1}\|\|\Gamma_J(\bar{u}_{|J}) - \Gamma_J(u_J)\| = \|\Gamma_J^{-1}\|\|\Gamma_J(\bar{u}_{|J}) - r_J\| \\
&= \|\Gamma_J^{-1}\|\|b(\bar{u}_{n_-}, \bar{u}_{n_+})\|.
\end{aligned}
$$

$\blacksquare$

In case of periodic boundary conditions, (27) reads,

$$\|\bar{u}_{|J} - u_J\| \leq C\|\bar{u}_{n_-} - \bar{u}_{n_+}\|.$$

The disadvantage of these boundary conditions obviously lies in the coupling of the end-points, which is not the case for projection boundary conditions. In numerical computations, this effect can clearly be observed, cf. Figure 8.
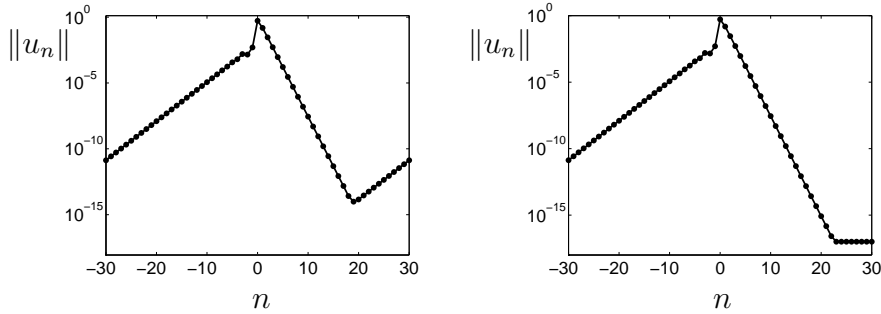

Figure 8: *Solution of (23) for the example from Section 3.3 on the finite interval $J = [-30, 30]$, with periodic (left) and projection boundary conditions (right).*

Combining Propositions 5 and 6, we prove for projection boundary conditions that approximation errors (27) decrease exponentially fast towards the middle of the interval J.

Proposition 7 *Assume **A1** and **A2**. Let u_J be the solution of $\Gamma_J u_J = r_J$ with projection boundary conditions (26), where $J = [n_-, n_+]$, $r_J := (0, \ldots, 0, r, 0, \ldots, 0)^T$, and $r \in \mathbb{R}^k$ is placed at N-th position, $n_- \leq N \leq n_+ - 1$. Then, a J-independent positive constant C exists, such that the following inequality for the error is satisfied:*

$$\|\bar{u}_n - u_n\| \leq C \left(e^{-\alpha_s(n-n_-)} e^{-\alpha_u(N-n_-)} + e^{-\alpha_u(n_+-n)} e^{-\alpha_s(n_+-N)} \right), \quad n \in J. \quad (28)$$

Proof: Applying Proposition 6 and the definition of the projection boundary operator (26), it follows that

$$\|\bar{u}_{|J} - u_J\| \leq C_1 \left\| \begin{pmatrix} Y_s^T \bar{u}_{n_-} \\ Y_u^T \bar{u}_{n_+} \end{pmatrix} \right\|. \quad (29)$$

Note that we get the same finite approximation for all sequences $B_{\mathbb{Z}}$ that coincide with $A_{\mathbb{Z}}$ on the finite interval J. On the other hand, the numerical approximation and the exact solution coincide on J, if the exact solution is a zero of the right hand side of (29), which means that the boundary operator is exact. Thus, the idea is, to construct a sequence $B_{\mathbb{Z}}$, fulfilling $B_{\hat{\jmath}} = A_{\hat{\jmath}}$, $\hat{J} = [n_- + 1, n_+ - 2]$, such that the exact solution $\bar{v}_{\mathbb{Z}}$ of $v_{n+1} = B_n v_n + \delta_{n,N} r$, $n \in \mathbb{Z}$ satisfies

$$Y_s^T \bar{v}_{n_-} = 0, \quad Y_u^T \bar{v}_{n_+} = 0.$$

Furthermore, we construct $B_{\mathbb{Z}}$, such that the homogeneous equation

$$u_{n+1} = B_n u_n, \quad n \in \mathbb{Z}$$

possesses an exponential dichotomy with J-independent rates α_s and α_u. The error is the difference between $\bar{u}_{|\hat{\jmath}}$ and $\bar{v}_{|\hat{\jmath}}$ for which, due to Proposition 5, the estimate

$$\|\bar{u}_n - \bar{v}_n\| \leq C \left(e^{-\alpha_s(n-n_--1)} e^{-\alpha_u(N-n_--1)} + e^{-\alpha_u(n_+-2-n)} e^{-\alpha_s(n_+-2-N)} \right), \quad n \in \hat{J}$$

holds and by adjusting the constant C, we obtain (28).

In the remaining part of the proof, we construct the sequence $B_{\mathbb{Z}}$. Let J be a finite interval and let P_n^s, P_n^u be the dichotomy projectors of (22) on J. Let A be a matrix with stable subspace $\mathcal{R}(Q^s)$ and unstable subspace $\mathcal{R}(Q^u)$, having in absolute value the largest stable and smallest unstable eigenvalues $\lambda_s = e^{-\alpha_s}$, $\lambda_u = e^{\alpha_u}$, respectively. Assuming that these eigenvalues are simple, $u_{n+1} = A_n u_n$ possesses an exponential dichotomy on $\mathbb{Z}$ with rates α_s and α_u.

We define the sequence $B_{\mathbb{Z}}$:

$$B_n := \begin{cases} A, & n \leq n_- - 1, \\ M_1, & n = n_-, \\ A_n, & n_- + 1 \leq n \leq n_+ - 2, \\ M_2, & n = n_+ - 1, \\ A, & n \geq n_+, \end{cases}$$

18

where M_1, M_2 have to be constructed. First note that

$$u_{n+1} = B_n u_n, \quad n \in \mathbb{Z} \tag{30}$$

has exponential dichotomies on $(-\infty, n_- - 1]$ and on $[n_+, \infty)$ with constant projectors $Q^{s,u}$, respectively. Thus this difference equation possesses an exponential dichotomy on $\mathbb{Z}$, with projectors $P_n^{s,u}$ on J, if the matrices $M_{1,2}$ connect the projectors from outside to the inside of J. By our assumptions, P_n^s and Q^s are projectors of equal rank, and therefore these projectors are similar. Finally, choose M_1, M_2 as described in Appendix A, Lemma 9, such that $M_1 Q^s M_1^{-1} = P_{n_-+1}^s$ and $M_2 P_{n_+-1}^s M_2^{-1} = Q^s$. Due to Lemma 10, the angle between the ranges of the dichotomy projectors P_n^s, P_n^u is bounded from below, and therefore, a J-independent constant $C > 0$ exists by Lemma 9, such that $\|M_{1,2}\|$, $\|M_{1,2}^{-1}\| \leq C$. These matrices connect the exponential dichotomy of the original equation (22) to the dichotomy of $u_{n+1} = A u_n$ and consequently, the resulting equation (30) possesses dichotomy constants that do not depend on the chosen interval J. The B-sequence possesses the following dichotomy projectors:

position n	$\ldots$	$n_- - 1$	n_-	$n_- + 1$	$\ldots$	$n_+ - 2$	$n_+ - 1$	n_+	$\ldots$
B_n	$\ldots$	A	M_1	A_{n_-+1}	$\ldots$	A_{n_+-2}	M_2	A	$\ldots$
projectors	$\ldots$	$Q^{s,u}$	$Q^{s,u}$	$P_{n_-+1}^{s,u}$	$\ldots$	$P_{n_+-2}^{s,u}$	$P_{n_+-1}^{s,u}$	$Q^{s,u}$	$\ldots$

Note that

$$Y_s^T \bar{v}_{n_-} = 0 \Leftrightarrow \bar{v}_{n_-} \in \mathcal{R}(Q^u) \quad \text{and} \quad Y_u^T \bar{v}_{n_+} = 0 \Leftrightarrow \bar{v}_{n_+} \in \mathcal{R}(Q^s)$$

which holds due to our construction. ∎

4.1.3 Approximation of dichotomy projectors

Using the above results, we introduce an algorithm that allows high accuracy approximations of dichotomy projectors.

Let $\Delta > 0$ be a given accuracy. For an $N \in \mathbb{N}$ we compute P_N^s as follows:

- Solve for $i = 1, \ldots, k$

$$u_{n+1}^i = A_n u_n^i + \delta_{n,N-1} e^i, \quad n \in J^i,$$

  where sufficiently large intervals J^i around N are chosen, using Proposition 7, such that the difference of exact and approximate solution is given as

$$\|\bar{u}_N^i - u_N^i\| \leq \Delta.$$

- Define

$$P_N^s := \left(u_N^1, \ldots, u_N^k \right),$$

  see Corollary 3.

Obviously, P_N^s approximates the exact dichotomy projector with accuracy Δ.

4.1.4 Approximation with exact boundary conditions

By computing the exact boundary operator first, we obtain an algorithm that gives high accuracy approximations of the solution of (5) on a given finite interval $J = [n_-, n_+]$:

- Approximate the dichotomy projectors $P_{n_-}^s$ and $P_{n_+}^u$ with accuracy Δ.

- Compute bases Y_s, Y_u of the orthogonal complement of $\mathcal{R}(P_{n_-}^u)$ and $\mathcal{R}(P_{n_+}^s)$, respectively, and define the boundary operator b_{opt} as in (26).

- Solve (23) with boundary operator b_{opt}.

Note that it requires solving $2k$ inhomogeneous equations on intervals around n_- and n_+, to get the two dichotomy projectors.

Denote by u_J the solution of (23) with boundary operator b_{opt}. By Proposition 6, the error can be estimated as

$$\|\bar{u}_{|J} - u_J\| \leq C \left\| \begin{pmatrix} Y_s^T \bar{u}_{n_-} \\ Y_u^T \bar{u}_{n_+} \end{pmatrix} \right\| \leq C\Delta \|\bar{u}_{n_-} + \bar{u}_{n_+}\|.$$

These results are illustrated in Figure 9 for the example from Section 3.6. As reference orbit $\bar{u}_{\mathbb{Z}}$, we take a long orbit segment of length $-n_-$, $n_+ = 10000$ which we compare with short segments u_J of length $n_- = -30$, $n_+ = 10$. In the left picture we take projection boundary conditions w.r.t. a fixed subspace. As one can see, the error decreases exponentially fast towards the middle, see Proposition 7. In the right of Figure 9, the error is plotted, when solving w.r.t. the exact boundary operator b_{opt}. In this case, errors are of magnitude 10^{-22}.
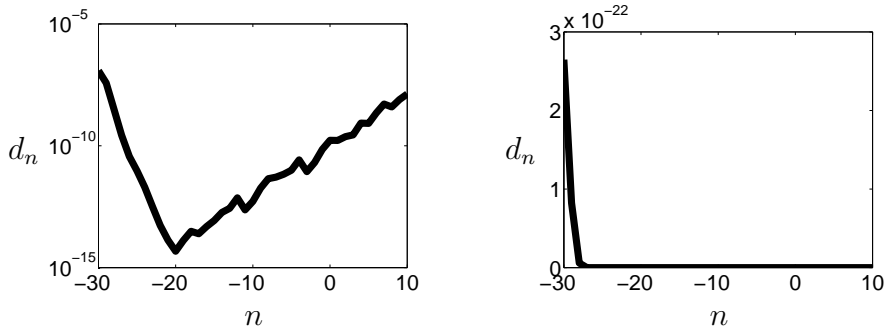

Figure 9: *Error $d_n = \|u_n - \bar{u}_n\|$ for projection boundary conditions w.r.t. fixed subspaces, and for the boundary operator b_{opt} that uses accurate approximations of dichotomy projectors (right).*

4.2 The least squares approach

Consider the inhomogeneous difference equation

$$u_{n+1} = A_n u_n + \delta_{n,0} r \tag{31}$$

and assume that the homogeneous equation possesses an exponential dichotomy on $\mathbb{Z}$, see **A1**. The unique bounded solution of (31) on $\mathbb{Z}$ is given as

$$\bar{u}_n = G(n,1)r, \quad \text{where} \quad G(n,1) = \begin{cases} -\Phi(n,1)P_1^u, & n < 1, \\ \Phi(n,1)P_1^s, & n \geq 1. \end{cases}$$

We prove that the difference between $\bar{u}_{\mathbb{Z}}$ and the least squares solution of (31) on the finite interval $J = [n_-, n_+]$, decreases exponentially fast to 0 as $-n_-, \, n_+ \to \infty$.

Theorem 8 *Assume **A1**. Denote by u_J the least squares solution of (31) on J. Then a J independent constant $C > 0$ exists, such that*

$$\|u_J - \bar{u}_{|J}\| \leq C \cdot (n_+ - n_-) \left(e^{\alpha n_-} + e^{-\alpha n_+} \right), \tag{32}$$

where $\alpha = \min\{\alpha_s, \alpha_u\}$.

Proof: Let B_n^s, B_n^u be orthonormal bases of $\mathcal{R}(P_n^s)$, $\mathcal{R}(P_n^u)$, and denote by k_s, k_u the dimensions of these subspaces. The general solution of (31) on J is

$$u_n = G(n,1)r + \Phi(n,n_-)B_{n_-}^s \eta + \Phi(n,n_+)B_{n_+}^u \zeta, \ n = n_-, \ldots, n_+, \ \eta \in \mathbb{R}^{k_s}, \ \zeta \in \mathbb{R}^{k_u}.$$

We find the minimal solution of (31) on J by computing the least squares solution of

$$F \begin{pmatrix} \eta \\ \zeta \end{pmatrix} := A \begin{pmatrix} \eta \\ \zeta \end{pmatrix} + b,$$

where

$$A = \begin{pmatrix} \Phi(n_-,n_-)B_{n_-}^s & \Phi(n_-,n_+)B_{n_+}^u \\ \vdots & \vdots \\ \Phi(n_+,n_-)B_{n_-}^s & \Phi(n_+,n_+)B_{n_+}^u \end{pmatrix}, \quad b = \begin{pmatrix} G(n_-,1) \\ \vdots \\ G(n_+,1) \end{pmatrix} r.$$

Note that A has rank k, therefore F is minimal for

$$\begin{pmatrix} \eta \\ \zeta \end{pmatrix} = -A^+ b = -(A^T A)^{-1} A^T b,$$

see [19], and the least squares solution of (31) on J, is given as

$$\begin{pmatrix} u_{n_-} \\ \vdots \\ u_{n_+} \end{pmatrix} = -A(A^T A)^{-1} A^T b + b.$$

21

We derive an estimate for the difference between $\bar{u}_{\mathbb{Z}}$ and least squares solution u_J:

$$\bar{u}_J - u_J = A(A^T A)^{-1} A^T b.$$

First it is shown that $A^T A$ has for all sufficiently large $-n_-$, n_+ a uniformly bounded inverse.

$$
\begin{aligned}
A^T A \;&=\; \begin{pmatrix} \sum_{i \in J} B_{n_-}^s{}^T \Phi(i, n_-)^T \Phi(i, n_-) B_{n_-}^s & \sum_{i \in J} B_{n_-}^s{}^T \Phi(i, n_-)^T \Phi(i, n_+) B_{n_+}^u \\ \sum_{i \in J} B_{n_+}^u{}^T \Phi(i, n_+)^T \Phi(i, n_-) B_{n_-}^s & \sum_{i \in J} B_{n_+}^u{}^T \Phi(i, n_+)^T \Phi(i, n_+) B_{n_+}^u \end{pmatrix} \\
&=: \begin{pmatrix} D_J^1 & N_J^1 \\ N_J^2 & D_J^2 \end{pmatrix}.
\end{aligned}
$$

The non-diagonal blocks tend exponentially fast to 0 as $J \to \mathbb{Z}$ since

$$
\begin{aligned}
\max\{\|N_J^1\|_2, \|N_J^2\|_2\} \;&\leq\; \sum_{i=n_-}^{n_+} K^2 \mathrm{e}^{-\alpha(i-n_-)} \mathrm{e}^{-\alpha(n_+-i)} \\
&=\; K^2 \sum_{i=n_-}^{n_+} \mathrm{e}^{-\alpha(n_+-n_-)} = K^2(n_+ - n_- + 1)\mathrm{e}^{-\alpha(n_+-n_-)}.
\end{aligned}
$$

The matrices D_J^1 and D_J^2 are uniformly bounded from above:

$$\|D_J^1\|_2 \leq K^2 \sum_{i=n_-}^{n_+} \mathrm{e}^{-2\alpha_s(i-n_-)} = K^2 \sum_{i=0}^{n_+-n_-} \mathrm{e}^{-2\alpha_s i} \leq K^2 \frac{1}{1-\mathrm{e}^{-2\alpha_s}},$$

and similarly $\|D_J^2\|_2 \leq K^2 \frac{1}{1-\mathrm{e}^{-2\alpha_u}}$. Furthermore $D_J^{1,2}$ are symmetric, positive definite matrices and $B_{n_\mp}^{s,u}$ are orthonormal bases, thus it follows that

$$
\begin{aligned}
K^2 \frac{1}{1-\mathrm{e}^{-2\alpha_s}} x^T x \;&\geq\; x^T D_{\mathbb{Z}}^1 x = \sum_{i=-\infty}^{\infty} x^T B_{n_-}^s{}^T \Phi(i, n_-)^T \Phi(i, n_-) B_{n_-}^s x \\
&\geq\; x^T B_{n_-}^s{}^T \Phi(n_-, n_-)^T \Phi(n_-, n_-) B_{n_-}^s x = x^T x, \\
K^2 \frac{1}{1-\mathrm{e}^{-2\alpha_u}} x^T x \;&\geq\; x^T D_{\mathbb{Z}}^2 x = \sum_{i=-\infty}^{\infty} x^T B_{n_+}^u{}^T \Phi(i, n_+)^T \Phi(i, n_+) B_{n_+}^u x \geq x^T x.
\end{aligned}
$$

As a consequence $A^T A$ is invertible for sufficiently large intervals J and has a uniformly bounded inverse.

Using the dichotomy estimates, one sees that

$$
\begin{aligned}
\|A\|_\infty \;&\leq\; \sup_{n \in J} \left(\|\Phi(n, n_-) B_{n_-}^s\|_2 + \|\Phi(n, n_+) B_{n_+}^u\|_2 \right) \\
&\leq\; \sup_{n \in J} \left(K\mathrm{e}^{-\alpha_s(n-n_-)} + K\mathrm{e}^{-\alpha_u(n_+-n)} \right) \\
&\leq\; K\mathrm{e}^{-\alpha_s} + K\mathrm{e}^{-\alpha_u} \leq C,
\end{aligned}
$$

22

where C does not depend on the interval J.

Denote by A_n the n-th block component of A. We derive an estimate for the n-th block component of $A(A^T A)^{-1} A^T b$:

$$\|A_n (A^T A)^{-1} A^T b\|_2 \le \|A_n\|_2 \|(A^T A)^{-1}\|_2 \|A^T b\|_2 \le C \|A^T b\|_2 \le C \sum_{\ell=n_-}^{n_+} \|\gamma_\ell\|_2$$

where

$$\gamma_\ell := \begin{pmatrix} (B_{n_-}^s)^T \Phi(\ell, n_-)^T \\ (B_{n_-}^u)^T \Phi(\ell, n_+)^T \end{pmatrix} \cdot G(l,1) r = \begin{pmatrix} (B_{n_-}^s)^T \Phi(\ell, n_-)^T \\ (B_{n_-}^u)^T \Phi(\ell, n_+)^T \end{pmatrix} \cdot \begin{cases} -\Phi(\ell,1) P_1^u r, & \ell \le 0, \\ \Phi(\ell,1) P_1^s r, & \ell \ge 1. \end{cases}$$

In case $\ell \le 0$ we get

$$
\begin{aligned}
\|\gamma_\ell\|_2 &\le K \left(e^{-\alpha(\ell - n_-)} + e^{-\alpha(n_+ - \ell)} \right) K e^{-\alpha(1-\ell)} \|r\|_2 \\
&= K^2 \left(e^{-\alpha(1-n_-)} + e^{-\alpha(n_+ - 2\ell + 1)} \right) \|r\|_2 \le K^2 \left(e^{\alpha(n_- -1)} + e^{-\alpha(n_+ +1)} \right) \|r\|_2,
\end{aligned}
$$

and similarly, it holds for $\ell \ge 1$

$$\|\gamma_\ell\|_2 \le K^2 \left(e^{\alpha(n_- +1)} + e^{-\alpha(n_+ -1)} \right) \|r\|_2.$$

As a consequence,

$$\|u_J - \bar{u}_{|J}\| = \|A_n (A^T A)^{-1} A^T b\| \le C \cdot (n_+ - n_-) \left(e^{\alpha n_-} + e^{-\alpha n_+} \right),$$

with some constant $C > 0$ that does not depend on n_- and n_+. ∎

Finally, we show numerically that the derived estimate for the error is quite sharp. We take the example from Section 3.3 for which the dichotomy rates are given in (18), choose symmetric intervals of the form $J = [-N, N]$ and compute a reference solution, by setting $N = 10000$. The differences of this solution to short least squares solutions for $N \in \{2, \dots, 50\}$ are shown in Figure 10 (black line). Neglecting constant terms, the approximation error (32) has the form $N e^{-\bar{\alpha}_u N}$, see the grey line in Figure 10.

In Figure 11 the error $d_n := \|\bar{u}_n - u_n\|$ between reference and least squares solution is plotted over n for $N \in \{5, 50, 200\}$.
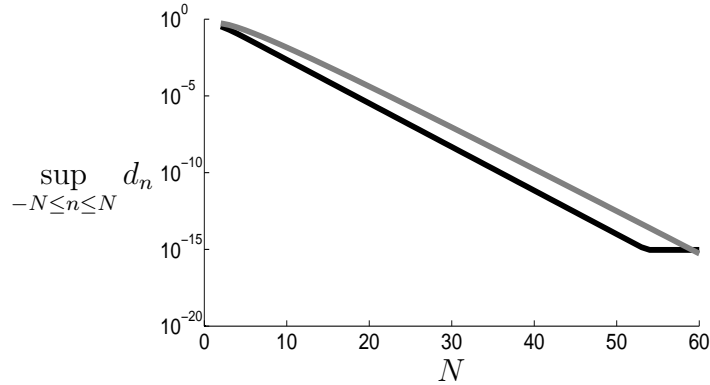
23

Figure 10: *Error of the least squares approach. Numerical results in black, theoretical estimates in grey.*
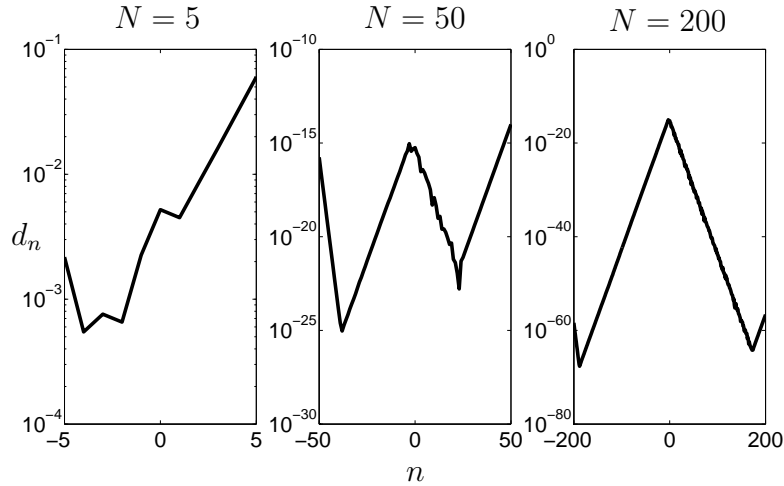

Figure 11: *Error $d_n = \|u_n - \bar{u}_n\|$ for $N \in \{5, 50, 200\}$, in different logarithmic scales.*

4.3   Conclusion

The approximation of dichotomy rates and projectors is based on computing bounded solutions of a specific inhomogeneous linear equation. For this task, we apply a boundary value and a least squares approach.

On the one hand, numerical experiments indicate that the least squares approach is twice as expensive as the boundary value ansatz.

On the other hand, well posedness of the boundary operator requires the extra assumption **A2**, which limits its applicability.

In both cases, estimates for the approximation error are introduced. The error

of the least squares solution is analyzed in Theorem 8:

$$\|u_J - \bar{u}_{|J}\| \leq C(n_+ - n_-)\left(e^{\alpha n_-} + e^{-\alpha n_+}\right).$$

For the boundary value approach, we get from Proposition 7 in case $N = 0$, $\alpha = \min\{\alpha_s, \alpha_u\}$:

$$\|u_n - \bar{u}_n\| \leq C\left(e^{-\alpha(n - 2n_-)} + e^{-\alpha(2n_+ - n)}\right), \quad n \in J,$$

and as a consequence

$$\|u_J - \bar{u}_{|J}\| \leq C\left(e^{\alpha n_-} + e^{-\alpha n_+}\right).$$

Thus, similar exponential estimates hold for both approaches.

A   Appendix

Some technical results, needed in Section 4.1.2 are presented in this appendix.

Lemma 9 *Fix $\sigma \in (0, \frac{\pi}{2}]$. Let A, B be two projectors in $\mathbb{R}^k$ with range A_s, B_s and nullspace A_u, B_u, respectively, where $\dim(A_s) = \dim(B_s)$, such that $\measuredangle(A_s, A_u) \geq \sigma$, $\measuredangle(B_s, B_u) \geq \sigma$.*

Then there exist a constant $C > 0$ that depends on σ but not on the specific choice of A, B, and an invertible matrix $T \in \mathbb{R}^{k,k}$, such that

$$T^{-1}AT = B, \quad \|T\| \leq C, \quad \|T^{-1}\| \leq C.$$

Proof: Let α_s, α_u, β_s, β_u be orthonormal bases of range and nullspace of A and B. We determine T uniquely as

$$T(\alpha_s) = \beta_s, \quad T(\alpha_u) = \beta_u.$$

Then each $x \in \mathbb{R}^k$ can be written in the form $x = \alpha_s \lambda_s + \alpha_u \lambda_u$, $\lambda_s \in \mathbb{R}^{\dim(A_s)}$, $\lambda_u \in \mathbb{R}^{\dim(A_u)}$ and thus, we get

$$\|T\|_2 = \sup_{x \in \mathbb{R}^k} \frac{\|Tx\|_2}{\|x\|_2} = \sup_{\lambda \in \mathbb{R}^k} \frac{\|T\alpha_s \lambda_s + T\alpha_u \lambda_u\|_2}{\|\alpha_s \lambda_s + \alpha_u \lambda_u\|_2} = \sup_{\lambda \in \mathbb{R}^k} \frac{\|\beta_s \lambda_s + \beta_u \lambda_u\|_2}{\|\alpha_s \lambda_s + \alpha_u \lambda_u\|_2}.$$

Note that

$$
\begin{aligned}
\|\beta_s \lambda_s + \beta_u \lambda_u\|_2^2 &= \|\lambda_s\|_2^2 + 2\lambda_s^T \beta_s^T \beta_u \lambda_u + \|\lambda_u\|_2^2 \\
&= \|\lambda_s\|_2^2 + \|\lambda_u\|_2^2 + 2\cos(\measuredangle(\beta_s \lambda_s, \beta_u \lambda_u))\|\beta_s \lambda_s\|_2 \|\beta_u \lambda_u\|_2 \\
&\leq \|\lambda_s\|_2^2 + \|\lambda_u\|_2^2 + 2\|\lambda_s\|_2 \|\lambda_u\|_2 \cos(\measuredangle(\beta_s, \beta_u)),
\end{aligned}
$$

and with $\varrho = \cos(\sigma) < 1$, it follows that

$$
\begin{aligned}
\|T\|_2^2 &\leq \sup_{\lambda \in \mathbb{R}^k} \frac{\|\lambda_s\|_2^2 + \|\lambda_u\|_2^2 + 2\varrho\|\lambda_s\|_2\|\lambda_u\|_2}{\|\lambda_s\|_2^2 + \|\lambda_u\|_2^2 - 2\varrho\|\lambda_s\|_2\|\lambda_u\|_2} \\
&= \sup_{\lambda \in \mathbb{R}^k} \frac{\frac{\|\lambda_s\|_2}{\|\lambda_u\|_2} + \frac{\|\lambda_u\|_2}{\|\lambda_s\|_2} + 2\varrho}{\frac{\|\lambda_s\|_2}{\|\lambda_u\|_2} + \frac{\|\lambda_u\|_2}{\|\lambda_s\|_2} - 2\varrho} \\
&= \sup_{x \in \mathbb{R}} \frac{|x| + \frac{1}{|x|} + 2\varrho}{|x| + \frac{1}{|x|} - 2\varrho} = \sup_{y \geq 2} \frac{y + 2\varrho}{y - 2\varrho} = \frac{1 + \varrho}{1 - \varrho} =: C.
\end{aligned}
$$

This finishes the proof, since the same estimate holds for T^{-1}.

∎

Lemma 10 *Let P be a projector. Assume $\measuredangle(\mathcal{R}(P), \mathcal{N}(P)) \to 0$ then $\|P\| \to \infty$.*

Proof: Let α, β be orthonormal bases of $\mathcal{R}(P)$, $\mathcal{N}(P)$, respectively. It holds

$$
\begin{aligned}
\|P\|_2 &= \sup_{x \in \mathbb{R}^k} \frac{\|Px\|_2}{\|x\|_2} = \sup_{\lambda \in \mathbb{R}^k} \frac{\|P\alpha\lambda_1 + P\beta\lambda_2\|_2}{\|\alpha\lambda_1 + \beta\lambda_2\|_2} \\
&= \sup_{\lambda \in \mathbb{R}^k} \frac{\|\lambda_1\|_2}{\|\alpha\lambda_1 + \beta\lambda_2\|}.
\end{aligned}
$$

Note that

$$
\|\alpha\lambda_1 + \beta\lambda_2\|_2^2 \geq \|\lambda_1\|_2^2 + \|\lambda_2\|_2^2 - 2\cos(\measuredangle(\alpha, \beta))\|\lambda_1\|_2\|\lambda_2\|_2,
$$

and with $\varrho = \cos(\measuredangle(\alpha, \beta))$, it follows that

$$
\begin{aligned}
\|P\|_2^2 &\leq \sup_{\lambda \in \mathbb{R}^k} \frac{\|\lambda_1\|_2^2}{\|\lambda_1\|_2^2 + \|\lambda_2\|_2^2 - 2\varrho\|\lambda_1\|_2\|\lambda_2\|_2} = \sup_{\lambda \in \mathbb{R}^k} \frac{\frac{\|\lambda_1\|_2}{\|\lambda_2\|_2}}{\frac{\|\lambda_1\|_2}{\|\lambda_2\|_2} + \frac{\|\lambda_2\|_2}{\|\lambda_1\|_2} - 2\varrho} \\
&= \sup_{x \in \mathbb{R}^+} \frac{x}{x + \frac{1}{x} - 2\varrho} = \frac{1}{1 - \varrho^2} \to \infty \text{ as } \varrho \to 1.
\end{aligned}
$$

∎

Lemma 11 *Assume $\boldsymbol{A2}$ and let the columns of Y_s form an orthonormal basis of $\mathcal{R}(Q^u)^\perp$. Then there exists for sufficiently large n, an n-independent constant $C > 0$ such that*

$$
\|Y_s^T x\| \geq C\|x\| \quad \text{for all } x \in \mathcal{R}(P_n^s).
$$

Proof: Let y be a column of Y_s, and let $x \in \mathcal{R}(P_n^s)$. It holds that

$$
\begin{aligned}
y^T x &= \|y\|_2\|x\|_2 \cos(\measuredangle(y, x)) \\
&\geq \|x\|_2 \cos(\measuredangle(\mathcal{R}(Q^u)^\perp, \mathcal{R}(P_n^s))) \geq \|x\|_2 \cos\sigma,
\end{aligned}
$$

since $\measuredangle(\mathcal{R}(Q^u)^\perp, \mathcal{R}(P_n^s)) \leq \sigma$, see $\boldsymbol{A2}$.

∎

Acknowledgement

References

[1] A. I. Alonso, J. Hong, and R. Obaya. Exponential dichotomy and trichotomy for difference equations. *Comput. Math. Appl.*, 38(1):41–49, 1999.

[2] W.-J. Beyn and T. Hüls. Error estimates for approximating non-hyperbolic heteroclinic orbits of maps. *Numer. Math.*, 99(2):289–323, 2004.

[3] W.-J. Beyn, T. Hüls, J.-M. Kleinkauf, and Y. Zou. Numerical analysis of degenerate connecting orbits for maps. *Internat. J. Bifur. Chaos Appl. Sci. Engrg.*, 14(10):3385–3407, 2004.

[4] W.-J. Beyn and J.-M. Kleinkauf. The numerical computation of homoclinic orbits for maps. *SIAM J. Numer. Anal.*, 34(3):1207–1236, 1997.

[5] S.-N. Chow and E. S. Van Vleck. A shadowing lemma approach to global error analysis for initial value ODEs. *SIAM J. Sci. Comput.*, 15(4):959–976, 1994.

[6] C. V. Coffman and J. J. Schäffer. Dichotomies for linear difference equations. *Math. Ann.*, 172:139–166, 1967.

[7] B. A. Coomes, H. Koçak, and K. J. Palmer. Rigorous computational shadowing of orbits of ordinary differential equations. *Numer. Math.*, 69(4):401–421, 1995.

[8] W. A. Coppel. *Dichotomies in Stability Theory*. Springer-Verlag, Berlin, 1978. Lecture Notes in Mathematics, Vol. 629.

[9] L. Dieci and E. S. Van Vleck. Lyapunov and Sacker-Sell spectral intervals. *J. Dynam. Differential Equations*, 19(2):265–293, 2007.

[10] G. H. Golub and C. F. Van Loan. *Matrix computations*. Johns Hopkins Studies in the Mathematical Sciences. Johns Hopkins University Press, Baltimore, MD, third edition, 1996.

[11] M. Hénon. A two-dimensional mapping with a strange attractor. *Comm. Math. Phys.*, 50(1):69–77, 1976.

[12] D. Henry. *Geometric Theory of Semilinear Parabolic Equations*. Springer-Verlag, Berlin, 1981.

[13] T. Hüls. Homoclinic orbits of non-autonomous maps and their approximation. *J. Difference Equ. Appl.*, 12(11):1103–1126, 2006.

[14] T. Hüls. Homoclinic trajectories of non-autonomous maps. Technical Report 07-011, Bielefeld University, CRC 701, 2007.

[15] J.-M. Kleinkauf. *Numerische Analyse tangentialer homokliner Orbits.* PhD thesis, Universität Bielefeld, 1998. Shaker Verlag, Aachen.

[16] K. J. Palmer. Exponential dichotomies, the shadowing lemma and transversal homoclinic points. In *Dynamics reported, Vol. 1*, pages 265–306. Teubner, Stuttgart, 1988.

[17] G. Papaschinopoulos. Exponential dichotomy for almost periodic linear difference equations. *Ann. Soc. Sci. Bruxelles Sér. I*, 102(1-2):19–28 (1989), 1988.

[18] C. Pötzsche and M. Rasmussen. Taylor approximation of invariant fiber bundles for nonautonomous difference equations. *Nonlinear Anal.*, 60(7):1303–1330, 2005.

[19] N. Shinozaki, M. Sibuya, and K. Tanabe. Numerical algorithms for the Moore-Penrose inverse of a matrix: direct methods. *Ann. Inst. Statist. Math.*, 24:193–203, 1972.